

Reactivity of Imidazole Derivatives toward Phosphate Triester in DMSO/Water Mixtures: A Comprehensive Study on the Solvent Effect

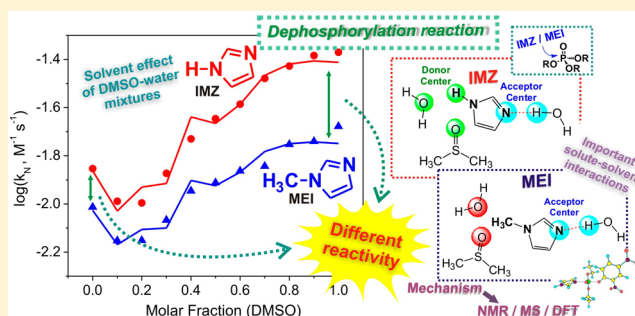
Renan B. Campos,^{‡,†} Everton H. Santos,[‡] Alfredo R. M. Oliveira,[‡] Fernanda Maria Marins Ocampos,[‡] Bruno S. Souza,[§] Andersson Barison,[‡] and Elisa S. Orth^{*,‡}

[‡]Departamento de Química, Universidade Federal do Paraná (UFPR), CP 19081, Curitiba, PR, CEP 81531-990, Brazil

[§]Universidade Federal de Santa Catarina, Florianópolis, SC, 88040-900, Brazil

S Supporting Information

ABSTRACT: Many imidazole (IMZ) derivatives of pharmaceutical interest, which are potentially catalytic in dephosphorylation reactions, are soluble solely in mixtures of water and organic solvent. In order to understand these poorly explored reactions and properly compare them, a thorough study related to solvent effects for the analogous spontaneous reaction and with common IMZ derivatives is necessary, which is lacking in the literature. Herein, we report a quantitative solvent effect analysis in DMSO/water mixtures for (i) the hydrolysis reaction of diethyl 2,4-dinitrophenylphosphate (DEDNPP) and (ii) the nucleophilic reaction of IMZ and 1-methylimidazole (MEI) with DEDNPP. The solvent effect was fitted satisfactorily with multiple regression analysis, correlating the obtained second-order rate constants with solvent parameters such as acidity, basicity, and polarity/polarizability from Catalán's scale. The contribution of these parameters can be taken into account to elucidate the reactivity in these media. Interestingly, IMZ is more reactive than MEI in DMSO, compared to water alone, which is attributed to the availability of hydrogen-bond formation. Nuclear magnetic resonance spectroscopy (¹H, ¹³C, and ³¹P), mass spectrometry, thermodynamic analysis, and density functional theory calculations were carried out to corroborate the proposed nucleophilic mechanism.



INTRODUCTION

Dephosphorylation reactions dictate many biologically important processes,^{1,2} and the extremely unfavorable P–O cleavage³ is accomplished by highly efficient enzymes. Enzymatic cleavage notwithstanding, the high stability of phosphate esters has made them useful in pesticides, insecticides, and chemical warfare.⁴ Hence, many studies have been dedicated to elucidating dephosphorylation reactions, especially those involving nucleophilic species, a benchmark to develop novel catalytic systems and to design artificial enzymes and efficient detoxification processes. In this context, imidazole (IMZ) stands out due to its outstanding and versatile catalysis, recurrent in enzymatic active sites. Increments over 10⁴-fold have been reported previously for IMZ with a series of phosphate esters.⁵ When mimicking the enzymatic environment, the use of nonaqueous solvents is an interesting approach,⁶ which is more truthful to the hydrophobic biological medium and broadens the possibilities for applications in biocatalysis.⁷

Solvent variations can drastically change the progress of a reaction, and since solvent–solute interactions are sensitive to the medium, understanding this complex phenomenon is not straightforward, although it has been extensively investigated. Some studies have relied on solvatochromic properties with widely used single-parameter scales, available for some specific

binary mixtures, such as $E_T(30)$,⁸ π^* ,^{9,10} α , and β .^{11,12} However, these scales are not available for all DMSO/water mixtures.

Gomez-Tagle et al.¹³ investigated the alkaline hydrolysis of phosphate esters in aqueous DMSO, acetonitrile, and dioxane mixtures¹³ and successfully correlated the medium effects with the kinetics parameters, using a recent scale based on a three-orthogonal-parameter treatment, allowing a comprehensive analysis. This scale takes into account acidity (SA), basicity (SB), and polarity/polarizability (SPP) parameters for different solvents mixtures, obtained from the studies by Catalán and co-workers.¹⁴ Similar methodology was adopted in a recent solvent effect study related to the aminolysis of dithiocarbonates.¹⁵

To the best of our knowledge, there are no studies reporting quantitative solvent effects in dephosphorylation reactions with IMZ derivatives, which is indubitably important when mimicking biological reactions in their complex environment. Further, many potentially catalytic IMZ derivatives of pharmaceutical interest are solubilized significantly only in organic media, and in order to comprehend these reactions, the solvent effect should foremost be understood. Little is known regarding the mechanism of action of these drugs, and related studies could enlighten researchers and also inform about

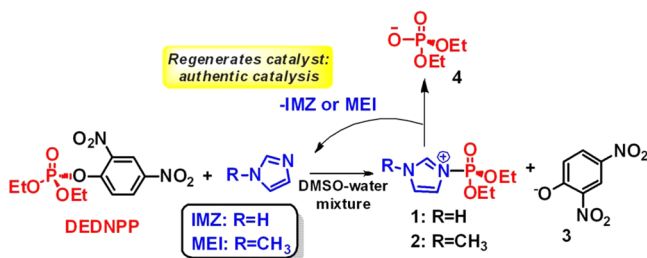
Received: May 23, 2015

Published: July 8, 2015



precautions needed with their administration. In addition, anomalous side effects could be elucidated, e.g., tumor incidence and mutagenic effect observed for metronidazole (antibiotic)¹⁶ and megazol (Chagas disease treatment),¹⁷ respectively. Herein, we report a thorough quantitative study of solvent effects based on Catalán's scale¹⁴ for the reactions of IMZ and its slightly more basic derivative 1-methylimidazole (MEI) with the reactive triester diethyl 2,4-dinitrophenylphosphate (DEDNPP) in DMSO/water mixtures. Scheme 1

Scheme 1. Representation of the Reactions Studied Herein



presents the proposed mechanism for the catalytic reactions evaluated, already elucidated for IMZ previously⁵ and to be analyzed here for MEI on the basis of 1D and 2D nuclear magnetic resonance spectroscopy (¹H, ¹³C, and ³¹P), mass spectrometry (MS), and analysis of thermodynamic parameters. Interestingly, an unexpected reactivity shift can be achieved by varying the solvent mixture. Density functional theory (DFT) calculations were also carried out to corroborate the proposed mechanism.

RESULTS AND DISCUSSION

Mechanistic Investigation by NMR. As previously reported for the reaction of IMZ with DEDNPP,⁵ we propose an analogous mechanism for MEI with DEDNPP, shown in Scheme 1, involving a rate-determining step of nucleophilic attack by the nitrogen on the phosphorus atom, leading to an intermediate (1 and 2), through a concerted pathway. For IMZ, the intermediate 1 is relatively stable and was characterized by 1D and 2D NMR analysis in a previous study.¹⁸ The analogous intermediate is unstable for MEI, since it cannot be stabilized by the loss of a proton, as reported by Jencks and co-workers in a study involving reactions of IMZ and derivatives with acetates.¹⁹

In this work, the reaction of MEI with DEDNPP was investigated by NMR spectroscopy, and typical consecutive ³¹P NMR spectra obtained are shown in Figure 1. The ³¹P{¹H} NMR spectrum of DEDNPP before reacting with MEI showed a signal at −7.5 ppm, as well as a small signal at 0.7 ppm, revealing the previous presence of a small amount of 4. The signal at −7.5 ppm could be unequivocally assigned to DEDNPP through ¹H–¹³C and ¹H–³¹P one-bond and long-range NMR correlation experiments (data given in Supporting Information). In this way, the aromatic hydrogens of DEDNPP at 8.98 (1H), 8.64 (1H), and 7.81 (1H) ppm as well as those from the ethoxy moieties at 4.39 (4H) and 1.39 (6H) ppm showed ¹H–³¹P long-range correlation with the same phosphorus at −7.5 ppm (Table 1). On the other hand, the phosphorus at 0.7 ppm showed ¹H–³¹P long-range correlation only with the hydrogens of the other ethoxy moiety observed in the ¹H NMR spectrum at 3.93 (4H) and 1.26 (6H) ppm, supporting the product 4 (Scheme 1).

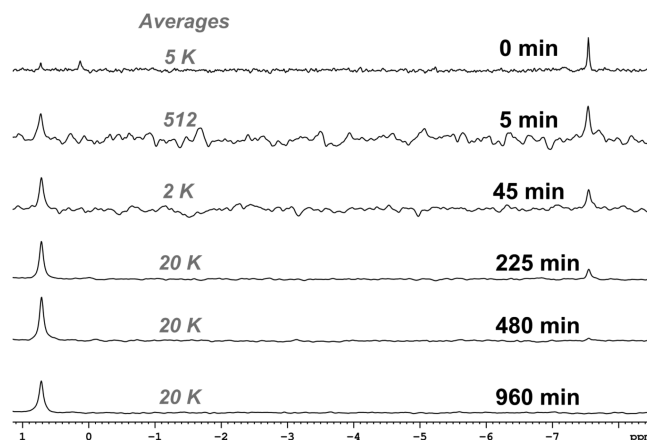


Figure 1. ³¹P{¹H} NMR spectra for the reaction of 1.5×10^{-4} M DEDNPP with 0.1 M MEI, pH 8.5, 25 °C.

Upon addition of DEDNPP to a MEI solution, the reaction products were followed by ³¹P{¹H} and ¹H NMR spectra. In the initial stages, the ³¹P{¹H} NMR spectra showed mainly the DEDNPP signal at −7.5 ppm, which decreased as the reaction progressed until 480 min. As a consequence, the signal at 0.7 ppm was enhanced during the reaction progress (Figure 1). It is interesting to notice that no other signals were observed in the ³¹P{¹H} and ¹H NMR spectra, revealing that if any reaction intermediates are formed, they are extremely unstable, as predicted previously. Additionally, as the reaction progressed, a second aromatic spin system emerged in the ¹H NMR spectra compared to those of DEDNPP, which did not show any ¹H–³¹P long-range NMR correlation; this was assigned to the product 3 (Scheme 1, Table 1). The overall ¹H, ¹³C, and ³¹P NMR chemical shift assignments are shown in Table 1, and all NMR spectra and correlation maps are given in the Supporting Information.

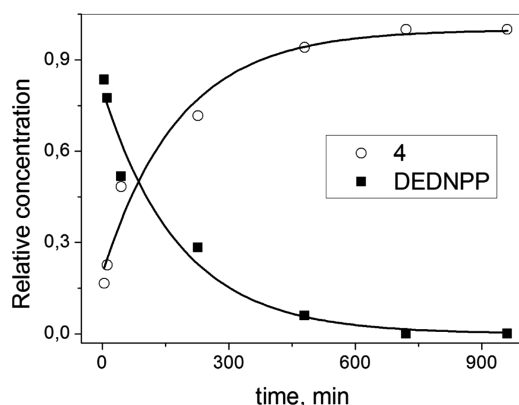
A profile of relative concentration vs reaction progress was obtained for the species detected by ³¹P NMR, given in Figure 2, which was fitted with equations for typical consecutive reactions.⁵ Herein, the rate constant for the consumption of DEDNPP by MEI ($\sim 9 \times 10^{-5} \text{ s}^{-1}$) agrees with the kinetic study (see Figure 4). Further, although the intermediate 2 was not detected by NMR, the formation of the species 4 results from the breakdown of the presumably unstable intermediate 2, corroborating the proposed mechanism. Thus, the intermediate decomposes rapidly, and its intrinsic rate constant is not distinguishable.

Mechanistic Investigation by MS. Since the phosphorylated MEI intermediate was not detected by NMR, MS analyses were performed. MS is known to be an interesting tool for mechanistic investigations.^{20,21} Our previous study, addressing the reaction of IMZ and DEDNPP, where the intermediate 1 was properly identified,⁵ validated the mechanism presented in Scheme 1 for IMZ.

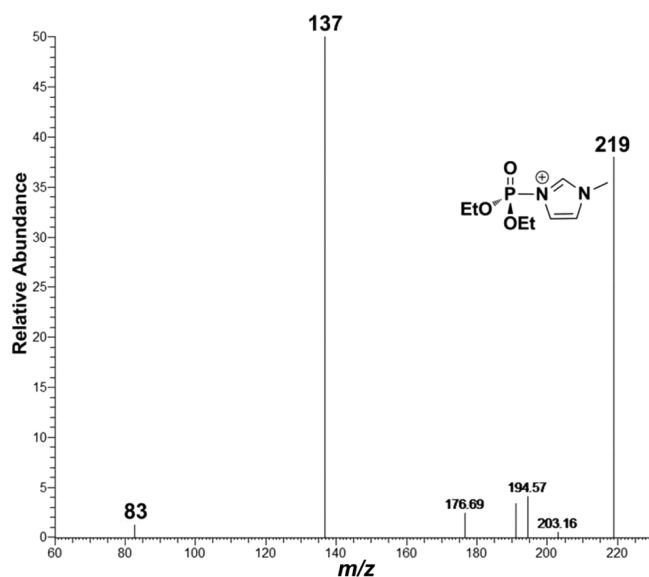
MS analysis carried out for the reaction of MEI and DEDNPP (aqueous medium at pH 8.5) in the negative- and positive-ion modes confirmed several key species in the proposed mechanism (data in Supporting Information). As expected, the ions of *m/z* 183 and 153 Da were detected in the negative-ion mode, assigned to the species 3 and 4 (Scheme 1). Moreover, spectra obtained in the positive-ion mode showed the presence of the ion of *m/z* 219 Da, attributed to intermediate 2, supporting the reaction pathway for MEI and

Table 1. NMR (600 MHz, H₂O/D₂O) Data for the Species Detected

compd	δ_{H}	δ_{C}	δ_{P}
MEI	3.79 (3H), 7.09 (1H), and 7.18 (1H)	33.9, 122.2, 127.0, and 138.7	
DEDNPP	8.98 (<i>dd</i> 2.8 and 0.9, 1H), 8.64 (<i>dd</i> 9.2 and 2.8, 1H), 7.81 (<i>dd</i> 9.2 and 1.0, 1H), 4.39 (<i>dq</i> 8.6 and 7.1, 4H), and 1.39 (<i>td</i> 7.1 and 1.2, 6H)	18.0, 69.9, 124.9, 126.5, 132.7, 143.4, 146.8, and 149.8	−7.5
3	8.89 (<i>d</i> 3.1, 1H), 8.12 (<i>dd</i> 9.6 and 3.1, 1H), and 6.75 (<i>d</i> 9.6, 1H)	127.9, 128.7, 132.0, 134.2, 138.9, and 173.7	
4	3.93 (<i>dq</i> 7.2 and 7.1, 4H) and 1.26 (<i>td</i> 7.1 and 0.6, 6H)	18.4 and 64.7	0.7

Figure 2. Relative concentration vs time for the species detected by ³¹P NMR, according to Scheme 1.

DEDNPP proposed in Scheme 1. Furthermore, the ion of *m/z* 219 Da was submitted to ESI-MS/MS (Figure 3), and its

Figure 3. ESI(+)-MS/MS spectrum of the ion of *m/z* 219 Da (2), detected for the reaction of MEI (0.5 M) and DEDNPP (2.5×10^{-5} M) at pH 8.5.

identity was confirmed by the loss of MEI moiety (*m/z* 83 Da), leading to the fragment of *m/z* 137 Da. These results corroborate the proposed mechanism and complement NMR analysis. Notably, the intermediate 2 has not been reported in the literature. Even in analogous studies involving acylation of MEI, the intermediate was not detected, and authors attribute this to the unstable nature of MEI-derived intermediates.²³ Hence, this is the first report that detects and characterizes the unstable intermediate 2 and furnishes evidence that reactions with MEI occur via the intermediate. This is an important

breakthrough, since many reports claim that the reaction of MEI should occur analogous to the reaction of IMZ, although there has been no clear evidence to confirm this.

Kinetic Profile for DMSO/Water Mixtures: Multi-Parameter Regression Solvent Effect Analyses. Once the proposed reactions were elucidated mechanistically (Scheme 1), we thoroughly analyzed the solvent effect, since it is surely correlated with the mechanism. The solvent effects of DMSO/water mixtures on the rate constants (k_{N}) for the reactions of DEDNPP with IMZ and MEI are presented in Figure 4. For comparison purposes, the rate constant for

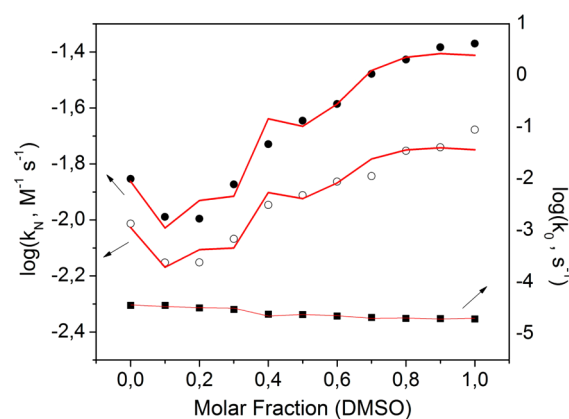


Figure 4. Rate constant dependence on the DMSO/water mixture for the reactions with DEDNPP at 25 °C. Left Y-axis: second-order rate constants of reaction of IMZ (●) and MEI (○). Right Y-axis: observed pseudo-first-order rate constant of the noncatalyzed spontaneous reaction of DEDNPP (■). The solid red lines refer to the multiple regression fitting according to eq 1.

spontaneous reaction of DEDNPP (k_0) was also determined at each DMSO/water composition, and ~2-fold enhancement was observed in pure water. These results are to some extent in agreement with the report by Mora and co-workers for the hydrolysis of phosphate triesters.²²

Furthermore, results evidence impressive catalytic activity for the nucleophiles in the reaction with DEDNPP in all solvent mixtures evaluated. Compared to the spontaneous reaction, improvements of up to 10^3 - and 5×10^2 -fold are observed for IMZ and MEI, respectively. These enhancements are typical for nucleophilic pathways (Scheme 1), confirmed herein by NMR and MS analysis and also by DFT calculations, as will be discussed later. Moreover, the nucleophilic reactions are more effective (higher k_{N}) in pure DMSO than in water, since, among other reasons, in the organic medium there is no possibility of hydrogen-bond donation by the solvent; thus, the solvent–solute attractive interaction has lower intensity compared with that in media containing water (fully discussed in the following). Another possible rationale is the higher molar fraction of the IMZ and MEI in DMSO than in water: a

solution containing 0.5 M concentration of the nucleophiles presents 0.0089 and 0.034 molar fraction in pure water and DMSO, respectively. Thus, the higher molar fraction could be associated with the increased reaction rate in pure DMSO solution compared to pure water. However, this rationale is misleading, since we would expect a progressive increase of k_{IMZ} or k_{MEI} with increasing DMSO composition, but this simple linear behavior was not observed herein. Likewise, both nucleophiles present an unusual lower rate constant from 10 to 30% DMSO. This behavior is similarly observed in other studies involving nucleophilic reactions in DMSO mixtures,¹³ and the anomaly around 20% has mainly been attributed to the solvent composition region presenting higher deviations from ideal solutions for DMSO/water mixtures.²³ Interestingly, in all binary mixture compositions, MEI presents lower rate constants than IMZ, even though it has a slightly higher $\text{p}K_{\text{a}}$ (7.21 for MEI and 6.95 for IMZ).²⁴ This apparent divergence may be caused by a minimal steric effect of the methyl group, contributing to less effective nucleophilic attack by MEI toward DEDNPP. This behavior has also been observed in acyl transfer reactions, and it was proposed that the similar reactivity of the two nucleophiles indicates that the nucleophilic attack is the rate-determining step, as proposed herein.²⁵ In contrast, if the breakdown of the intermediate was slow, possibly involving proton transfer from the N–H group (Scheme 1), higher rate constants would be expected for the reaction involving MEI.²³ Furthermore, a possible general base catalysis by a second IMZ molecule (not possible with MEI), commonly observed for phosphate and acetate ester hydrolysis,^{26,27} has not been considered herein as an important pathway. This is according to previous results⁵ that showed a deuterium isotope effect of ~ 1 for the reaction of IMZ with DEDNPP in aqueous media, whereas that value would typically be higher than 2 for general base catalysis.²⁸ Also, general base catalysis is more important with substrates with poor leaving groups,²⁶ and DEDNPP has a good leaving group, 3 ($\text{p}K_{\text{a}}^{\text{LG}} = 4.07$).²⁹ Surprisingly, we propose in the following that the reactivity ratio between IMZ and MEI can be varied by changing the solvent mixture medium.

The solvent effect for the nucleophilic reactions (IMZ and MEI) presented in Figure 4 was fitted and quantified on the basis of a nonlinear multi-parameter regression analysis, described by eq 1,¹³ using Catalan's scale of SA, SB, and SPP

$$\log k_{\text{N}} = \log k_{\text{g}} + A(\text{SA}) + B(\text{SB}) + P(\text{SPP}) \quad (1)$$

parameters for different solvents mixtures (values used are given in the Supporting Information).¹⁴ In eq 1, k_{N} is the experimental second-order rate constant for the nucleophilic reactions, k_{g} is an independent term, and the coefficients A , B , and P indicate the contribution of each parameter, SA, SB, and SPP, respectively. Other equations (eqs 2–7, Table 2) were also proposed to describe the experimental data, which were obtained from eq 1 by neglecting the contributions of the SA, SB, and SPP parameters, separately and/or concomitantly. Although our focus is on the nucleophilic reactions, we also fitted the data for the spontaneous reaction, i.e., hydrolysis of DEDNPP in Figure 4 with eq 1, in order to confirm that the method is also valid for the spontaneous reaction. Nevertheless, Table 2 presents the fitting parameters obtained using eqs 1–7 for the hydrolysis reaction (only best fit) and also for reactions with IMZ and MEI, along with statistical values, used to infer

Table 2. Parameters Obtained with the Multi-Parameter Regression Analysis for the Reaction of DEDNPP with IMZ and MEI in DMSO/Water Mixtures^a

eq	$\log k_{\text{g}}$	A	B	P	R^2	F^b
Hydrolysis Reaction						
1	−6.54 (0.66)	0.74 (0.15)	0.67 (0.22)	1.34 (0.52)	0.95	58.4
Reaction with IMZ						
1	6.98 (1.60)	−2.82 (0.37)	−3.39 (0.55)	−6.00 (1.27)	0.96	77.8
2	−4.40 (1.65)	—	0.68 (0.34)	2.44 (1.77)	0.61	8.8
3	−0.51 (0.44)	−1.29 (0.34)	−1.38 (0.66)	—	0.82	24.4
4	−1.56 (1.94)	−0.58 (0.19)	—	0.12 (1.89)	0.73	14.3
5	−6.43 (1.48)	—	—	4.81 (1.5)	0.48	9.4
6	−2.13 (0.13)	—	1.00 (0.26)	—	0.57	14.2
7	−1.43 (0.05)	−0.59 (0.10)	—	—	0.76	32.2
Reaction with MEI						
1	4.45 (1.40)	−2.06 (0.32)	−2.57 (0.48)	−4.38 (1.11)	0.92	40.6
2	−3.90 (1.23)	—	0.41 (0.26)	1.80 (1.32)	0.54	6.8
3	−1.03 (0.33)	−0.95 (0.27)	−1.10 (0.50)	—	0.78	18.8
4	−2.02 (1.51)	−0.37 (0.15)	—	0.26 (1.47)	0.65	10.4
5	−5.13 (1.04)	—	—	3.24 (1.06)	0.46	10.3
6	−2.22 (0.10)	—	0.65 (0.20)	—	0.49	10.7
7	−1.76 (0.04)	−0.39 (0.08)	—	—	0.69	23.2

^aErrors are presented between parentheses. “—” indicates the parameter was neglected from eq 1 for the given equation. ^bParameter obtained from variance analysis based on F distribution; higher values indicate better statistical results.³⁰

which equation best describes the solvent effect behavior observed.

Indubitably, Table 2 evidences that, for both nucleophiles, fitting with single-parameter equations (eqs 5–7, neglecting two of the terms from eq 1) presents poor statistical results based on errors, correlation coefficient (R^2), and statistical F , especially for SB and SPP parameters. Double-parameter fitting (eqs 2–4, neglecting one of the terms from eq 1) presents slightly better correlation but still with unacceptable errors, mainly for SPP parameter. Likewise, both SA and SB parameters are important to describe the solvent–solutes interactions. Nonetheless, these parameters need to be combined with SPP parameter: fits with eq 3 (only SA and SB contribute) presents large errors and poor statistical coefficient in contrast to eq 1 (all parameters contribute). Finally, results using all three parameters SA, SB, and SPP (eq 1) are the most statistically satisfactory, with relatively low errors and good correlation coefficient for both nucleophiles, shown in Figure 4 by the solid lines. It should be noted that sometimes fewer parameters are needed for satisfying fits, e.g., with only two parameters.¹³

Consistently, only parameters obtained from fitting with eq 1 were analyzed herein, which best describes the solvent effect in Figure 4, also adopted in similar reports.^{13,15} For the nucleophilic reactions, the negative coefficients obtained for all three parameters in eq 1 indicate that they contribute decreasing the rate constant (Table 2). The most significant contribution for lowering the reaction rate is SPP (P coefficient) pointing that the medium polarity stabilizes the reagents and probably also the transition states, although this is expected since water, DMSO, and the binary mixtures present high and similar values of polarity/polarizability parameter ($SPP^{\text{water}} = 1.00$ and $SPP^{\text{DMSO}} = 0.962$, given in Supporting Information). The negative coefficient A for the SA parameter indicates stabilization of both nucleophiles receiving hydrogen bonds from the medium, i.e., decreasing k_N values,¹³ which is more pronounced with IMZ than MEI: -2.83 and -2.06 , respectively. This difference may be attributed to the inherent tautomerism in IMZ providing a more susceptible hydrogen-bond receptor site, not observed in MEI. Similarly, for the SB parameter, the negative coefficient B evidences that both nucleophiles are stabilized by donating a hydrogen bond to the medium. Again, this effect is more pronounced for IMZ, attributed to the N–H group (absent in MEI) contributing to the strong hydrogen-bonding with the medium. Above 20% DMSO/water mixture, both nucleophilic reaction rates (IMZ and MEI) are enhanced, concomitant with an increase of SB and decrease of SA; thus, SB is the main factor governing the reaction, as indicated by the B coefficient (Table 2 and Catalán's scale¹⁴ in the Supporting Information). Moreover, above 40% DMSO, SB is higher than SA, indicating that the hydrogen-bond-accepting nature of the solvent mixture contributes to enhancing the rate of reactions relative to water-rich mixture compositions. Finally, multiple regressions fitting based on the three Catalán's parameters implies that solvation of reactants is an important tool to understand the reaction rates and guide discussions.

The values for $\log k_g$ (Table 2) are associated with the reaction occurring in the gas phase in which all three coefficients of SA, SB, and SPP equal to zero. The positive $\log k_g$ values shown in Table 2 states that the nucleophilic reactions studied are faster in gas phase, consistent with former reports for alkaline dephosphorylation reactions.¹³ Particularly, rate constants in the gas phase are up to 9.4×10^8 - and 3.91×10^6 -fold higher for IMZ and MEI, respectively, than in solution (considering 20% molar fraction of DMSO). Although these results seem overestimated, they corroborate the hypotheses that reactants are stabilized by the medium, disfavoring the nucleophilic reactions evaluated, and evidently, in a general analysis, the signs of all coefficients A , B , P , and $\log k_g$ point to this. This is also consistent with the rate-determinant step of the nucleophilic attack on the phosphorus center, leading to the phosphorylated intermediate, shown in Scheme 1.

Best statistical fitting results for the hydrolysis reaction of DEDNPP were also obtained using three parameters (eq 1) to describe the medium; these coefficients are also shown in Table 2. Accordingly, the hydrolysis reaction would be at least 10^6 -fold slower in the gas phase compared to any composition of aqueous DMSO, and SA, SB, and SPP parameters contribute to a favorable reaction, since the coefficients A , B , and P are positive, and these results agree with the earlier cited report by Mora and co-workers,²² where many water molecules are involved in the phosphotriester hydrolysis.

In order to account for the nucleophiles' reactivity difference on the basis of the solvent mixture, the most relevant rate constants ratios are given in Table 3. As mentioned previously,

Table 3. Most Relevant Rate Constants Ratios in Different Solvent Mixtures^a

solvent mixture (DMSO/water)	k_{IMZ}/k_0	k_{MEI}/k_0	$k_{\text{IMZ}}/k_{\text{MEI}}$
100% water	194.7	134.7	1.44
20% DMSO	158.4	110.6	1.43
100% DMSO	1072.4	527.6	2.03

^aIn s^{-1} with 0.5 M of the nucleophiles.

both nucleophiles exhibit high catalytic activity compared with the spontaneous reaction in the corresponding solvent composition. It is clear that in DMSO the nucleophiles show the highest catalytic activities, and in 20% DMSO/water, both become considerably less reactive. Except for 20% molar fraction of DMSO, the ratio of $k_{\text{IMZ}}/k_{\text{MEI}}$ is enhanced with increasing DMSO content. Thus, while the hydrogen-bond capacity of the medium decreases (DMSO-rich mixtures), the nucleophilic activity of IMZ is magnified, in contrast to MEI. Moreover, in water-rich mixtures, the nucleophiles behave similarly, and the similar reaction rates and these behaviors can be explained on the basis of solute–solvent interactions.

Understanding the nucleophiles' reactivity difference on the basis of the solvent mixture is mainly rationalized by hydrogen-bonding, as depicted in Figure 5. IMZ is a receiver/donor of hydrogen bonds (N: and N–H moieties), and consequently the attractive interaction of IMZ with water is intensified, compared to that of MEI (N: and N–Me nitrogen sites). Thus, IMZ nucleophilic activity increases in DMSO-rich medium, since lacking hydrogen bonds with water improves its nucleophilic power. Since DMSO behaves as a hydrogen-bond acceptor, increasing composition of this solvent entails to an increase of IMZ–DMSO–IMZ clusters (two IMZ donating hydrogen bonds to the oxygen of DMSO, Figure 5). It is reasonable to imply that this interaction is weaker than in a similar case of water–IMZ–water (water behaving as a hydrogen-bond acceptor), since k_{IMZ} in DMSO is slightly higher than in water. The basicity of medium is more important than acidity to decrease the rate of nucleophilic reaction of IMZ when compared with MEI (B coefficient -3.39 and -2.57 , respectively, Table 2). Based on these results and associated with the hydrogen-bond-donating from IMZ to DMSO, it leads to the consideration that IMZ could present even higher reactivity in a less hydrogen-bond-accepting solvent. Compared to IMZ, MEI presents less contribution of the SA, SB, and SPP parameters (Table 2), and the absence of N–H hydrogen-bond-donating capacity suggests that MEI is less intensely solvated in any DMSO/water composition and consequently less influenced by medium variations. As a consequence, IMZ is 3.04 times more reactive in DMSO than in water, while for MEI this ratio is only 2.16.

Overall, results evidence that the nucleophilic reactivity of IMZ and MEI can be enhanced by the solvent mixture. Surely, this is an important tool for designing prominent catalytic systems based on enzymatic active sites. Also, this elucidation furnishes a better understanding for analogous reactions with pharmaceuticals derived from IMZ, in which their potential catalytic mechanism could correlate to side effects or even incite precaution with its administration.

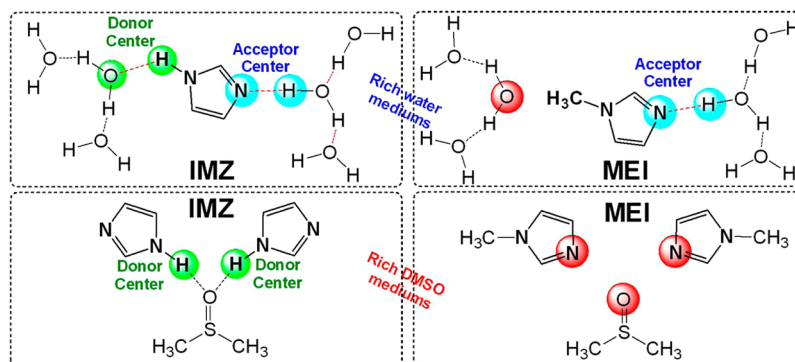


Figure 5. Hydrogen bond formation of IMZ and MEI in water-rich and DMSO-rich compositions.

Thermodynamic Analysis. Thermodynamic parameters were obtained for three binary solvent mixture compositions: 0, 20, and 100% DMSO, which presented the most interesting ratios shown in Table 3. Four temperatures were chosen (288, 298, 308, and 318 K) for the Eyring plot (given in Supporting Information) of each chosen solvent composition, and the resulting activation parameters are shown in Table 4.

Table 4. Thermodynamic Parameters for the Reactions of IMZ and MEI with DEDNPP in Different Solvent Compositions^a

DMSO		ΔH^\ddagger , kcal mol ⁻¹	ΔS^\ddagger , cal K ⁻¹ mol ⁻¹	ΔG^\ddagger , kcal mol ⁻¹
0%	IMZ	7.7	-42.6	20.4
	MEI	9.58	-37.0	20.6
20%	IMZ	8.74	-39.4	20.5
	MEI	10.4	-34.8	20.8
100%	IMZ	6.85	-43.2	19.7
	MEI	7.79	-40.7	19.9

^aAt 298 K. Experimental data, linear plots, and equations used are given in the Supporting Information.

The large and negative entropies of activation⁵ are in agreement with nucleophilic catalysis and corroborate NMR and DFT calculation results (*vide infra*) indicating that IMZ and MEI follow the same reaction mechanism with DEDNPP. Lu and co-workers studied DMSO/water mixtures on the basis of the enthalpy and entropy of activation for dielectric relaxation.³¹ These two parameters are larger in the range of 0.15–0.4 DMSO molar fraction, compared with pure water, which was attributed to the stronger hydrogen-bonding between water and DMSO than between two water molecules. Moreover, in 0.33 DMSO molar fraction there is the

stoichiometric formation of H₂O–DMSO–H₂O complex, with the organic solvent acting as an acceptor of hydrogen bonds by oxygen.³¹ In this range, the solution presents the most homogeneous charge distribution, and it may have a relation with the disfavoring of the reaction between DEDNPP and IMZ/MEI in 10–30% DMSO/water compositions. Despite the similarity of ΔG^\ddagger for the reactions (Table 4) evaluated, the contributions of the thermodynamic parameters differ. Moreover, the activation enthalpy of both nucleophilic reactions increases when the mixture increases from 0 to 20% DMSO and decreases in 100% DMSO, resembling the results of enthalpy of activation for dielectric relaxation for DMSO/water mixtures which follows the same behavior,³¹ although entropy contribution is not clear.

Mechanistic Investigation by DFT Calculations. As indicated by NMR, MS, and thermodynamic analysis, the mechanism for the reaction of IMZ and MEI with DEDNPP follows a nucleophilic pathway. Nevertheless, DFT calculations represent an important tool for providing detailed information on whether the aminolysis of the triester occurs by concerted S_N2(P) or a two-step mechanism. Accordingly, calculations were performed for the cleavage of DEDNPP on the basis of the nucleophilic attack of the free nitrogen atom of IMZ or MEI on the phosphorus atom. The polarizable continuum model (PCM) was used to simulate the solvent effect without the inclusion of explicit solvation, since the spontaneous (much slower) reaction can be neglected and the deuterium isotope effect is very low. Calculations were obtained in water and DMSO medium, although since the solvent effect could not be distinguished by the theoretical methodology adopted, most data are given in the Supporting Information, and here we focus on the novelty of the mechanistic confirmation (in water),

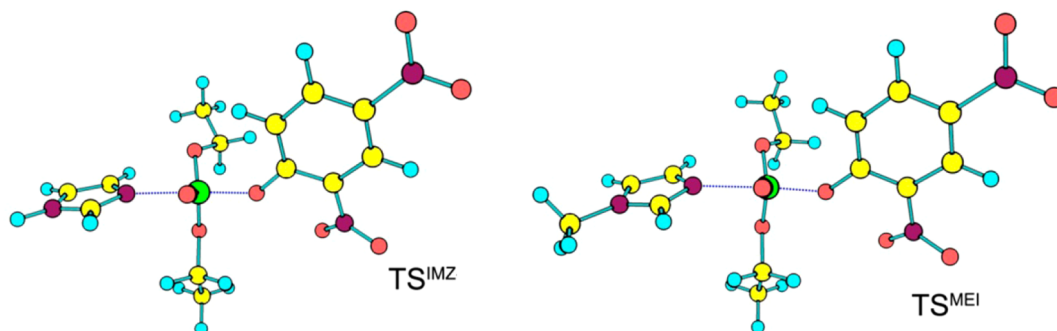
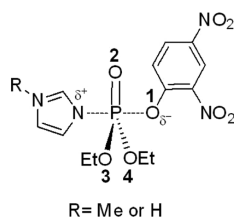


Figure 6. Transition states for the S_N2(P) reaction of IMZ and MEI with DEDNPP.

which has not been reported for dephosphorylation reactions with IMZ derivatives.

Figure 6 shows the structure of the transition states found for the aminolysis of DEDNPP with IMZ (TS^{IMZ}) and MEI (TS^{MEI}), and the main geometrical parameters are given in Table 5. (The optimization data in DMSO are given in the

Table 5. Interatomic Distances (Å) and Dihedral Angle (deg) for the $\text{S}_{\text{N}}2(\text{P})$ Aminolysis of DEDNPP in Water^a



structure	N–P	P–O1	P–O2	P–O3	P–O4	C ^b –N–P–O2
TS^{IMZ}	2.248	1.792	1.493	1.592	1.597	21.69
TS^{MEI}	2.261	1.789	1.493	1.591	1.597	30.52
DEDNPP		1.642	1.483	1.586	1.583	
IMZ-INT	1.753		1.482	1.575	1.579	0.62
MEI-INT	1.747		1.482	1.576	1.580	0.65

^aGeometrical parameters for DEDNPP are given for comparison. Same data for reactions in DMSO are given in the Supporting Information. ^bC2 of IMZ, between nitrogen atoms.

Supporting Information.) Both TS structures IMZ/MEI and leaving group are roughly collinear, with an N–P–O1 interatomic angle of about 7°.

As shown in Figure 7 for both nucleophiles, intrinsic reaction coordinate (IRC) analyses indicate that no stable pentacoordinate intermediate is involved in the reaction coordinate. Thus, all reactions studied involve a classical $\text{S}_{\text{N}}2(\text{P})$ mechanism, corroborating the kinetic analysis discussed earlier, and moreover, these results are in accordance with previous results for alkaline hydrolysis of dimethylphosphate triesters³² which involves a pentacoordinate intermediate only for compounds with poor leaving groups ($\text{p}K_{\text{a, LG}} > 8$). The theoretical energies are quite similar for both nucleophiles in both reaction media and do not reproduce well the solvent effect differences determined by the experimental results. Thus, as expected, the PCM cannot describe the solvent effect observed in the kinetic study, and probably explicit solvent molecules are necessary since specific solvent–solute interactions play an important role in these reactions. Notwithstanding, IRC data for IMZ and MEI in both media are presented in Figure 7 to highlight the concerted pathway of the studied reactions.

Moreover, the calculated free energies of activation for the $\text{S}_{\text{N}}2(\text{P})$ reactions for IMZ and MEI, 22.2 and 21.7 kcal mol^{−1} in water, respectively, are in relative agreement with the experimental results (data for DMSO given in Supporting Information), but cannot explain the nucleophile's reactivity (IMZ > MEI). Although the energy difference is discrete (even experimental values are similar, Table 4), this can be attributed to the failure in finding complexes between IMZ or MEI and DEDNPP which are more stable than the free reactants. Therefore, the values are relative to isolated reactants. Nonetheless, calculation results were fundamental to corroborate the nucleophilic pathway by a concerted mechanism for the reactions of both nucleophiles with DEDNPP, which agrees with all results presented herein.

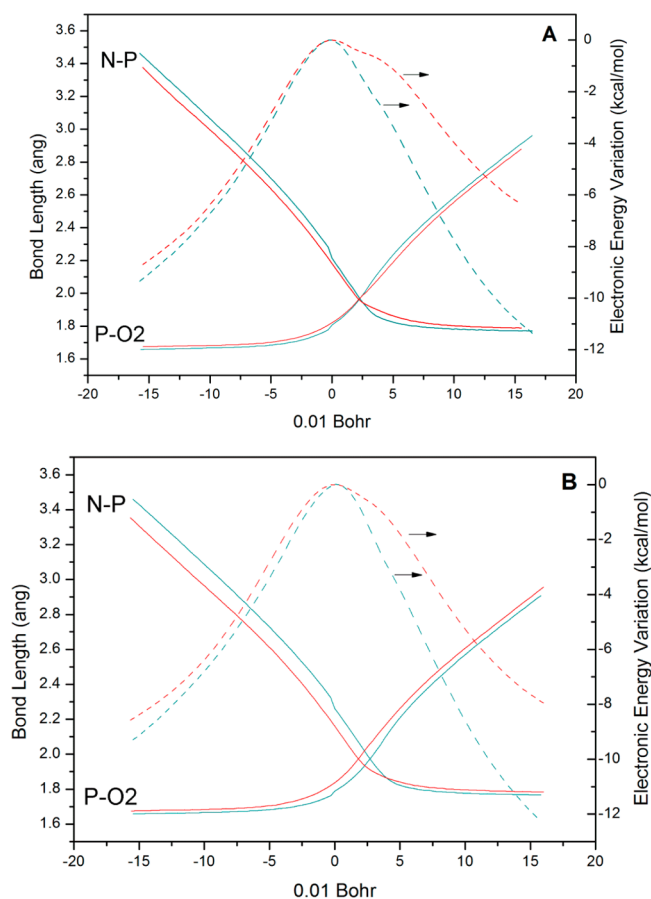


Figure 7. IRC graphs for aminolysis of DEDNPP with IMZ (A) and MEI (B) showing the variation of N–P and P–O2 interatomic distances in water (blue) and DMSO (red). Also shown is the electronic energy variation in relation to the TS energy (dashed lines).

CONCLUSION

The solvent effect on the reactivity of IMZ and MEI toward DEDNPP was thoroughly investigated in different DMSO/water compositions on the basis of a quantitative medium analysis using a multiple nonlinear regression method. First, the proposed nucleophilic pathway was corroborated by NMR and MS analysis for MEI, previously experimentally elucidated for IMZ.⁵ Interestingly, the IMZ-phosphorylated intermediate in the reaction of MEI, known to be unstable and previously not reported, was detected herein by MS.

The combination of the three solvent parameters SA, SB, and SPP from Catalán's scale¹⁴ successfully described the nucleophilic and hydrolysis rate profiles. On this basis, hydrolysis of DEDNPP is disfavored in the gas phase since the transition state of this reaction is supported by surrounding hydrogen-bonded waters, and we suggest that this arrangement is most favored in the liquid phase. On the other hand, nucleophilic reactions involving IMZ and MEI are much slower in the liquid phase. Based on positive A, B, and P coefficients, this suggests that SA, SB, and SPP contribute to decrease the rate of both reactions, and these results confirm that solvent–solute interactions are important to understand the reaction progress. Due to its molecular structure, in water-rich mixtures, IMZ can act as both donor and acceptor of hydrogen bonds, which considerably decreases its reactivity. However, in DMSO-rich compositions, the resulting solute–solvent interactions are less attractive, yielding higher reaction rates.

Compared to IMZ, the lower reaction rates of MEI in all solvent compositions can be attributed to the absence of tautomerism due to the presence of a methyl group rather than hydrogen, which makes MEI a less versatile nucleophile, even though it has a higher pK_a . Additionally, thermodynamic parameters were obtained, which are in consonance with the proposed nucleophilic mechanism for both reactions due to the large and negative entropies of activation. Moreover, theoretical calculations emphasize that IMZ and MEI reactions with DEDNPP follow a nucleophilic concerted pathway.

Overall, the reactivity of IMZ derivatives of pharmaceutical interest, that require nonaqueous medium, can be explored in different medium compositions considering the analysis presented herein. Important information that enables proper comparisons has been elucidated and concomitantly incited related quantitative studies regarding solvent effects.

■ EXPERIMENTAL SECTION

Materials. DMSO 99.9%, IMZ, and MEI were obtained commercially. Solutions were prepared immediately before use. DEDNPP was prepared as described in the literature.⁵

Kinetic Measurements. The reactions were performed by adding 10 μL of a 1.5 mmol L^{-1} stock solutions of DEDNPP in acetonitrile (ACN) into 3 mL of a 0.5 mol L^{-1} solution of IMZ or MEI, prepared in different proportion of DMSO/water (0–100% DMSO). Pseudo-first-order conditions were maintained, and the appearance of the phenolate 3 was monitored spectrophotometrically at 400 nm. The temperatures of cuvettes during the reactions were controlled with a thermostatted cell holder. Plots of absorbance against time were used to calculate the observed first-order rate constants (k_{obs}) with an iterative least-squares software. All the correlation coefficients were higher than 0.99. Second-order rate constants (k_N , eq 8) of reactions evolving nucleophiles IMZ and MEI with DEDNPP in different compositions of the binary mixture DMSO–water were determined.

$$k_{\text{obs}} = k_0 + k_N[\text{Nucleophile}] \quad (8)$$

NMR Analysis. Kinetic experiments were followed through NMR by adding an aliquot of DEDNPP in ACN to a MEI solution in H_2O directly into NMR tubes, and ^{31}P and ^1H spectra were acquired during reaction evolution, until there were no alterations on the signal intensities. In order to follow the changes on the concentration of the species during reaction, the signal areas for each species in the $^{31}\text{P}\{^1\text{H}\}$ NMR were determined with aid of Bruker ERETIC approach. For this, the area of the signal from a known concentration triphenyl phosphate solution, acquired at same conditions as in reaction spectra, was used as reference and employed to find signal areas of all species in all other ^{31}P NMR spectra.

The ^1H and ^{31}P spectra as well as one-bond and long-range ^1H – ^{13}C and ^1H – ^{31}P correlation experiments were acquired in H_2O /ACN containing some D_2O drops, at 303 K on a 400 NMR spectrometer operating at 9.4 T, observing ^{31}P and ^1H nucleus at 161.98 and 400.13 MHz, respectively. The spectrometer was equipped with a 5 mm direct detection multinuclear probe with z-gradient. ^1H NMR chemical shifts are given in ppm related to TMS (3-(trimethylsilyl) propionic-2,2,3,3- d_4 acid, sodium salt) signal at 0.00 ppm as internal reference, while those of ^{31}P NMR are related to H_3PO_4 (85% in D_2O) signal from a capillary reference.

MS Analysis. Mass spectrometry analyses were performed on a Linear Ion Trap Mass Spectrometer, equipped with an ESI ion source. Typically, reactions were analyzed with MEI (0.5 M) and DEDNPP (2.5×10^{-5} M) in aqueous medium at pH 8.5, in the negative and positive ion modes. Main conditions: curtain gas nitrogen flow, 20 mL min^{-1} ; ion spray voltage, –4500 eV; declustering potential, –21 eV; entrance potential, –10 eV; and collision cell exit potential, –12 eV. Main species were subjected to ESI-MS/MS by collision-induced

dissociation (CID) with helium, and collision energies ranged from 5 to 35 eV.

DFT Calculations. DFT calculations for the nucleophilic attack of IMZ and MEI on DEDNPP were performed at the B3LYP/6-311++G(d,p) level of theory using Gaussian 09³³ implemented in linux operating systems. The water and DMSO environments were simulated with the PCM using the integral equation formalism variant (IEFPCM) with radii and non-electrostatic terms for the SMD solvation model reported by Truhlar and co-workers.³⁴ The default converge parameters were used for all calculations. Frequency calculations were performed at 1 atm and 298.15 K. Reactants and products were identified by the absence of imaginary frequencies whereas transition states showed one single imaginary frequency. IRC³⁵ were computed to confirm the reaction paths. The step size is given in units of 0.01 Bohr as implemented in Gaussian 09. For conversion from 1 atm standard state to 1 mol L^{-1} standard state, ΔG^\ddagger was corrected by subtracting 1.90 kcal mol^{-1} from the calculated value according to an $\text{A} + \text{B} \rightarrow \text{C}$ reaction.^{36,37}

■ ASSOCIATED CONTENT

§ Supporting Information

Kinetic data, Eyring plot, Cartesian coordinates of the TS, optimization and energy data for the reactions in DMSO, and further ^1H , $^{31}\text{P}\{^1\text{H}\}$ NMR spectra, as well as one-bond and long-range ^1H – ^{13}C and ^1H – ^{31}P NMR correlation maps and MS data. The Supporting Information is available free of charge on the ACS Publications website at DOI: 10.1021/acs.joc.5b01152.

■ AUTHOR INFORMATION

Corresponding Author

*E-mail: elisaorth@ufpr.br.

Present Address

[†]R.B.C.: Departamento de Química e Biologia, Universidade Tecnológica Federal do Paraná, Curitiba, PR, 80230-901, Brazil

Notes

The authors declare no competing financial interest.

■ ACKNOWLEDGMENTS

The authors acknowledge financial support from CNPq, INCT-Catálise, CAPES, Fundação Araucária, UFPR, and UTFPR.

■ REFERENCES

- (1) Westheimer, F. H. *Science* **1987**, 235, 1173.
- (2) Westheimer, F. H. *Abstr. Pap. Am. Chem. Soc.* **1997**, 214, 126.
- (3) Wolfenden, R. *Chem. Rev.* **2006**, 106, 3379.
- (4) Yang, Y. C.; Baker, J. A.; Ward, J. R. *Chem. Rev.* **1992**, 92, 1729.
- (5) Orth, E. S.; Wanderlind, E. H.; Medeiros, M.; Oliveira, P. S. M.; Vaz, B. G.; Eberlin, M. N.; Kirby, A. J.; Nome, F. J. *Org. Chem.* **2011**, 76, 8003.
- (6) Neverov, A. A.; Brown, R. S. *Inorg. Chem.* **2001**, 40, 3588.
- (7) Khmel'nitsky, Y. L.; Rich, J. O. *Curr. Opin. Chem. Biol.* **1999**, 3, 47.
- (8) Dimroth, K.; Bohlmann, F.; Reichard, C.; Siepmann, T. *Liebigs Ann. Chem.* **1963**, 661, 1.
- (9) Jones, M. E.; Taft, R. W.; Kamlet, M. J. *J. Am. Chem. Soc.* **1977**, 99, 8452.
- (10) Kamlet, M. J.; Abboud, J. L.; Taft, R. W. *J. Am. Chem. Soc.* **1977**, 99, 6027.
- (11) Kamlet, M. J.; Taft, R. W. *J. Am. Chem. Soc.* **1976**, 98, 377.
- (12) Taft, R. W.; Kamlet, M. J. *J. Am. Chem. Soc.* **1976**, 98, 2886.
- (13) Gomez-Tagle, P.; Vargas-Zuniga, I.; Taran, O.; Yatsimirsky, A. K. *J. Org. Chem.* **2006**, 71, 9713.
- (14) Catalán, J.; Diaz, C.; Garcia-Blanco, F. J. *Org. Chem.* **2001**, 66, 5846.
- (15) Millan, D.; Santos, J. G.; Castro, E. A. *J. Phys. Org. Chem.* **2012**, 25, 989.

- (16) Rustia, M.; Shubik, P. *J. Natl. Cancer Inst.* **1972**, *48*, 721.
- (17) Poli, P.; de Mello, M. A.; Buschini, A.; Mortara, R. A.; de Albuquerque, C. N.; da Silva, S.; Rossi, C.; Zucchi, T. M. A. D. *Biochem. Pharmacol.* **2002**, *64*, 1617.
- (18) Orth, E. S.; Almeida, T. G.; Silva, V. B.; Oliveira, A. R. M.; Ocampos, F. M. M.; Barison, A. J. *Mol. Catal. A: Chem.* **2015**, *403*, 93.
- (19) Kirsch, J. F.; Jencks, W. P. *J. Am. Chem. Soc.* **1964**, *86*, 833.
- (20) Coelho, F.; Eberlin, M. N. *Angew. Chem., Int. Ed.* **2011**, *50*, 5261.
- (21) Rodrigues, T. S.; Silva, V. H. C.; Lalli, P. M.; de Oliveira, H. C. B.; da Silva, W. A.; Coelho, F.; Eberlin, M. N.; Neto, B. A. D. *J. Org. Chem.* **2014**, *79*, 5239.
- (22) Mora, J. R.; Kirby, A. J.; Nome, F. *J. Org. Chem.* **2012**, *77*, 7061.
- (23) Wong, D. B.; Sokolowsky, K. P.; El-Barghouthi, M. I.; Fenn, E. E.; Giammanco, C. H.; Sturlaugson, A. L.; Fayer, M. D. *J. Phys. Chem. B* **2012**, *116*, 5479.
- (24) Lenarcik, B.; Ojczenasz, P. *J. Heterocycl. Chem.* **2002**, *39*, 287.
- (25) Jencks, W. P.; Carriuolo, J. *J. Biol. Chem.* **1959**, *234*, 1272.
- (26) Neuvonen, H. *J. Chem. Soc., Perkin Trans. 2* **1995**, 951.
- (27) Neuvonen, H. *J. Chem. Soc., Perkin Trans. 2* **1987**, 159.
- (28) Kirby, A. J.; Medeiros, M.; Oliveira, P. S. M.; Brandao, T. A. S.; Nome, F. *Chem. - Eur. J.* **2009**, *15*, 8475.
- (29) Medeiros, M.; Orth, E. S.; Manfredi, A. M.; Pavez, P.; Micke, G. A.; Kirby, A. J.; Nome, F. *J. Org. Chem.* **2012**, *77*, 10907.
- (30) Miller, R. G. *Beyond ANOVA, basics of applied statistics*; Wiley: New York, 1986.
- (31) Lu, Z. J.; Manias, E.; Macdonald, D. D.; Lanagan, M. *J. Phys. Chem. A* **2009**, *113*, 12207.
- (32) Tarrat, N. *J. Mol. Struct.: THEOCHEM* **2010**, *941*, 56.
- (33) Frisch, M. J.; Trucks, G. W.; Schlegel, H. B.; Scuseria, G. E.; Robb, M. A.; Cheeseman, J. R.; Scalmani, G.; Barone, V.; Mennucci, B.; Petersson, G. A.; Nakatsuji, H.; Caricato, M.; Li, X.; Hratchian, H. P.; Izmaylov, A. F.; Bloino, J.; Zheng, G.; Sonnenberg, J. L.; Hada, M.; Ehara, M.; Toyota, K.; Fukuda, R.; Hasegawa, J.; Ishida, M.; Nakajima, T.; Honda, Y.; Kitao, O.; Nakai, H.; Vreven, T.; Montgomery, J. A., Jr.; Peralta, J. E.; Ogliaro, F.; Bearpark, M.; Heyd, J. J.; Brothers, E.; Kudin, K. N.; Staroverov, V. N.; Kobayashi, R.; Normand, J.; Raghavachari, K.; Rendell, A.; Burant, J. C.; Iyengar, S. S.; Tomasi, J.; Cossi, M.; Rega, N.; Millam, N. J.; Klene, M.; Knox, J. E.; Cross, J. B.; Bakken, V.; Adamo, C.; Jaramillo, J.; Gomperts, R.; Stratmann, R. E.; Yazyev, O.; Austin, A. J.; Cammi, R.; Pomelli, C.; Ochterski, J. W.; Martin, R. L.; Morokuma, K.; Zakrzewski, V. G.; Voth, G. A.; Salvador, P.; Dannenberg, J. J.; Dapprich, S.; Daniels, A. D.; Farkas, Ö.; Foresman, J. B.; Ortiz, J. V.; Cioslowski, J.; Fox, D. J. *Gaussian 09*; Gaussian, Inc.: Wallingford, CT, 2009.
- (34) Marenich, A. V.; Cramer, C. J.; Truhlar, D. G. *J. Phys. Chem. B* **2009**, *113*, 6378.
- (35) Fukui, K. *Acc. Chem. Res.* **1981**, *14*, 363.
- (36) Benson, S. *Thermochemical Kinetics*; Wiley: New York, 1968.
- (37) Rastelli, A.; Bagatti, M.; Gandolfi, R. *J. Am. Chem. Soc.* **1995**, *117*, 4965.